In-situ spectroscopy of intrinsic Bi_2Te_3 topological insulator thin films and impact of extrinsic defects: Supplementary Information

P. Ngabonziza,[1] R. Heimbuch,[1] N. de Jong,[2] R. A. Klaassen,[1] M. P. Stehno,[1] M. Snelder,[1] A. Solmaz,[1] S. V. Ramankutty,[2] E. Frantzeskakis,[2] E. van Heumen,[2] G. Koster,[1] M. S. Golden,[2] H. J. W. Zandvliet,[1] and A. Brinkman[1]

[1] *Faculty of Science and Technology and MESA+ Institute for Nanotechnology, University of Twente, 7500 AE Enschede, The Netherlands*
[2] *Van der Waals-Zeeman Institute, University of Amsterdam, Science Park 904, 1098 XH, Amsterdam, Netherlands*

(Dated: June 15, 2015)

PACS numbers: 79.60.Dp, 73.20.-r, 68.37.Ef, 79.60.-i

I. XPS MEASUREMENTS

X-ray photoemission spectroscopy (XPS) spectra were taken *in-situ* using an Omicron Nanotechnology system equipped with a monochromatic aluminum source (Kα x-ray source XM1000) with a photon energy of 1486.7 eV. The background pressure was $\sim 5 \times 10^{-11}$ mbar. The kinetic energy of electrons emitted from the sample were analyzed using a 7 channel EA 125 electron analyzer operated in CAE mode. XPS measurements were performed a few hours after film growth, with the films having remained in UHV at all times.

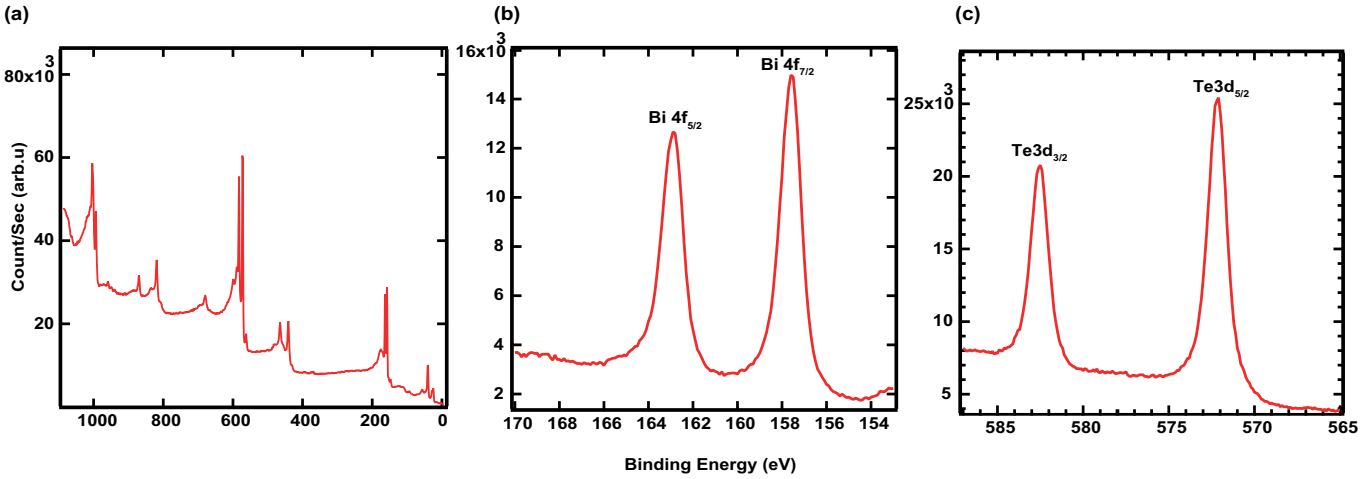

Figure S1: (color on-line) *In-situ* XPS measurement on a 20 nm Bi_2Te_3 film grown on sapphire that was subsequently measured in ARPES experiment (see Fig. 3(b)). (a) Survey scan taken a few hours after the film growth. Only Bi and Te peaks are resolved. (b) and (c) High-resolution scans around the Bi $4f$ and Te $3d$ main peaks, respectively

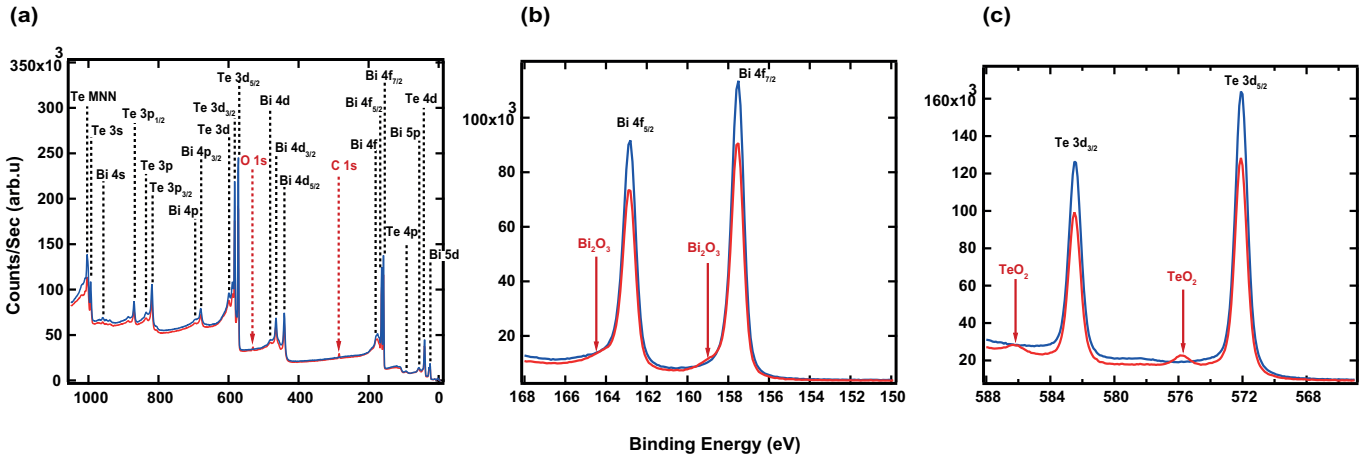

Figure S2: (color on-line) Effect of *ex-situ* exposure on a 30 nm Bi_2Te_3 film grown on sapphire. (a) An XPS survey scan when the sample is measured *in-situ* (blue) and after being exposed to ambient conditions (red). After *ex-situ* exposure, oxygen and carbon peaks appear. High resolution Bi $4f$ (b) and Te $3d$ (c) XPS spectra before and after short exposure. After exposure, there is a clear formation of a TeO_2 layer, whereas Bi_2O_3 formation is barely noticeable. This is consistent with the fact that the surface in an ideal crystal is terminated by tellurium atoms[1]. The bismuth oxidation would be expected to become significant, after the tellurium outer layer has been completely oxidized.

II. XRD MEASUREMENTS

To further characterize our films, additional *ex-situ* x-ray diffraction (XRD) measurements were done, which indicated the high crystalline quality of our Bi_2Te_3 films, grown using the two-step procedure described in the main body of the paper. We show below XRD data of a 30 nm film grown on Al_2O_3 [0001] and a 15 nm film grown on STO [111]. The film on sapphire was measured at low temperature using STM/STS, whereas the film on STO was measured using ARPES (See main text).

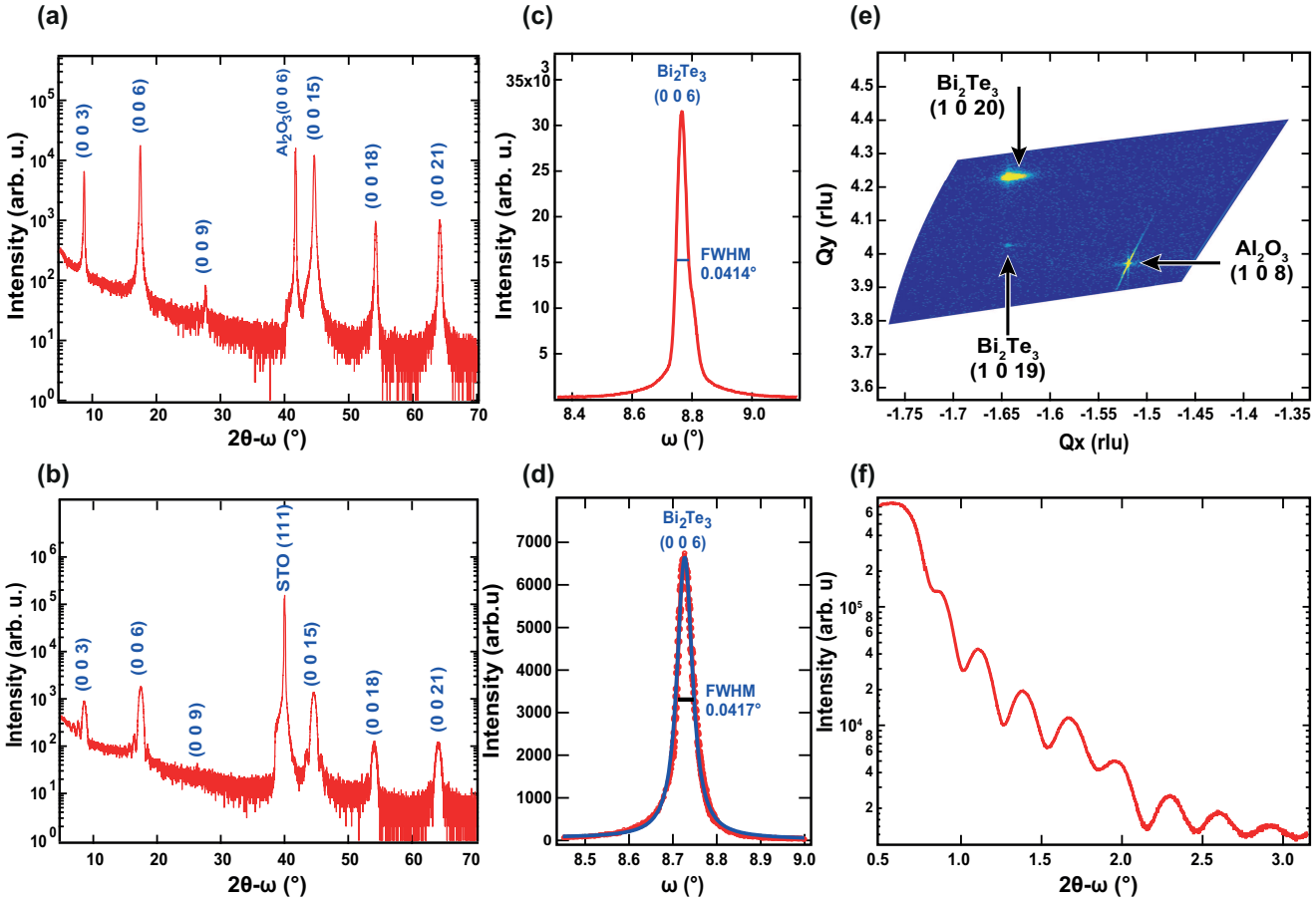

.eps

Figure S3: (color on-line) *Ex-situ* XRD measurements. (a) and (b): $2\theta - \omega$ scans of Bi_2Te_3 films grown on sapphire and STO. Only the substrate peaks and the (0 0 3) family of Bi_2Te_3 diffraction peaks are resolved. (c) and (d): Rocking curves of the Bi_2Te_3 main peak at (0 0 6). (e) A 2D reciprocal space map of a 30 nm film grown on sapphire. Positions of the Al_2O_3 (1 0 8) and Bi_2Te_3 (1 0 20) and (1 0 19) peaks are shown. (f) X-ray reflectivity data of a 15 nm film grown on STO showing distinct Kiessig fringes over more than five orders of magnitude in intensity. Despite the significant lattice mismatch between the film and substrates[2,3], high structural-quality films are grown.

III. MODEL CALCULATION OF DENSITY OF STATES AND DISPERSION RELATIONS

To model Bi_2Te_3 dispersion relations along the $\overline{\Gamma} - \overline{M}$ and $\overline{\Gamma} - \overline{K}$ directions, we used the k·p Hamiltonian described in Ref.[1,4] to calculate the Green's function and subsequently the Density Of States (DOS). This model includes anisotropic higher order terms, for example describing the outward bending of the Dirac cone along the $\overline{\Gamma} - \overline{M}$ direction at the energy close to the maximum of the valence band, also present in ab-initio calculations[4]. We used as few parameters as possible to describe the measured ARPES dispersions. The parameters used are (in the same notation as Ref.[4]): $m_1^* = $ -0.054 $eV^{-1}\dot{A}^{-2}$, $v = 2.55\ eV\dot{A}$, $\alpha = 5.5\ eV\dot{A}^2$, $\lambda = 250\ eV\dot{A}^3$ and the chemical potential $\mu = 225\ meV$ above the Dirac point, which coincides with the data from the STS experiments. The Green's function was calculated on a grid of 1200 × 1200 k-points with an energy step of 3 meV. Figure S4 (a) and (b) show the spectral functions obtained by summing the imaginary parts of the diagonal components of the Green's function. The DOS, shown as inset in Fig. 3 (a) in the main text, was obtained by integrating the spectral functions over the Brillouin zone.

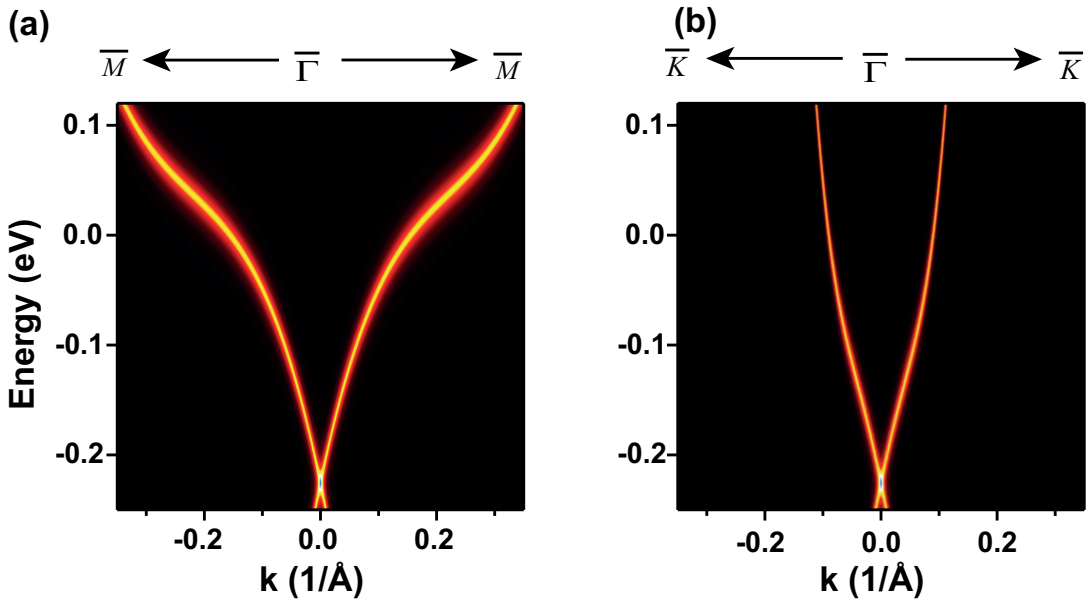

Figure S4: (color on-line) Calculated spectral functions of Bi_2Te_3 along the (a) $\overline{\Gamma} - \overline{M}$ and (b) $\overline{\Gamma} - \overline{K}$ directions. Outward bending of the Dirac cone is observed only along the $\overline{\Gamma} - \overline{M}$ direction.

IV. STM SPECTROSCOPY BEFORE AND AFTER EXPOSURE TO AMBIENT CONDITIONS

To investigate the impact of exposure to ambient conditions, the 30 nm Bi_2Te_3 film grown on sapphire was exposed for 10 minutes to ambient conditions, then loaded back into the STM chamber. After this procedure, we took several topography images at different positions on the exposed surface. We used the same setpoint parameters as for the spectra discussed in the main text. The differential conductance curves before and after atmospheric exposure are plotted together below. Clear changes in the general shape of the spectra are observed, as was also the case for the ARPES spectra of the film exposed to air (Fig. 5 (b) in the main text and related discussions).

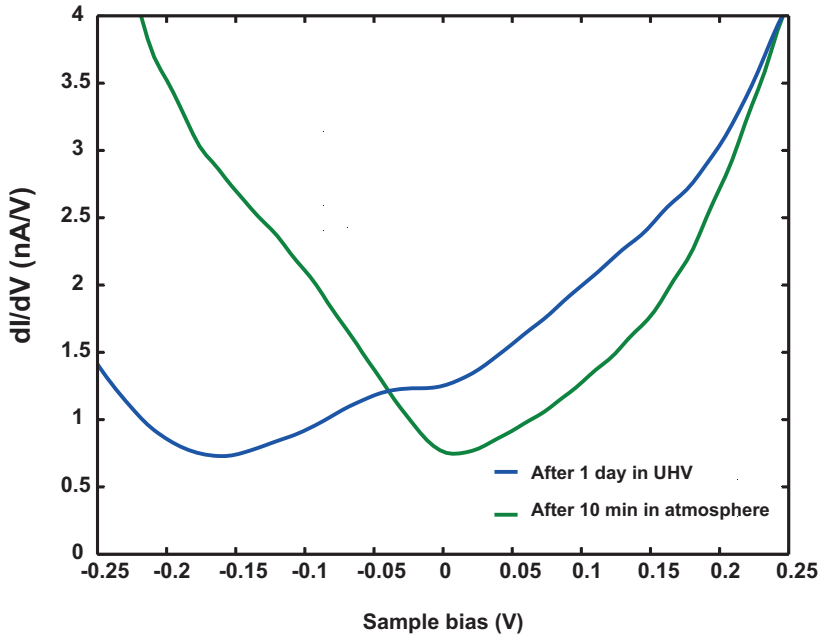

Figure S5: (color on-line) Conductance spectra of a film exposed for 10 min to ambient (air) conditions. Before exposure (blue) and after exposure (green). The region previously associated with linearly dispersing surface bands is absent in the exposed sample, highlighting the deterioration of surface states after exposure to ambient conditions as observed in the ARPES data (see Fig. 5(b) in the main text).

V. ARPES MEASUREMENTS

ARPES spectra in the vicinity of the Fermi level were also acquired on Bi_2Te_3 films grown on $SrTiO_3$ [111] substrates. The spectra were taken both at low ($\sim$ 17K) and room temperature using a Scienta VUV5000 helium photon source of 21.2 eV photon energy (He I line) and 40.8 eV (He II line) for valence band spectra; and a Scienta 2002 hemispherical electron analyzer.

Figure S6 (a) shows an illustrative ARPES spectra of a 15 nm Bi_2Te_3 film grown on STO in two steps growth at a substrate temperatures of 190°C (first layer) and 250°C (second layer). Spectra were taken at low temperature. Only topological surface states intersecting the Fermi level are observed for this sample also. To investigate the effect of UHV exposure on the electronic structure of these films, we performed ARPES measurements over different time intervals in UHV condition, with the results shown in Fig. S6 (a)-(d).

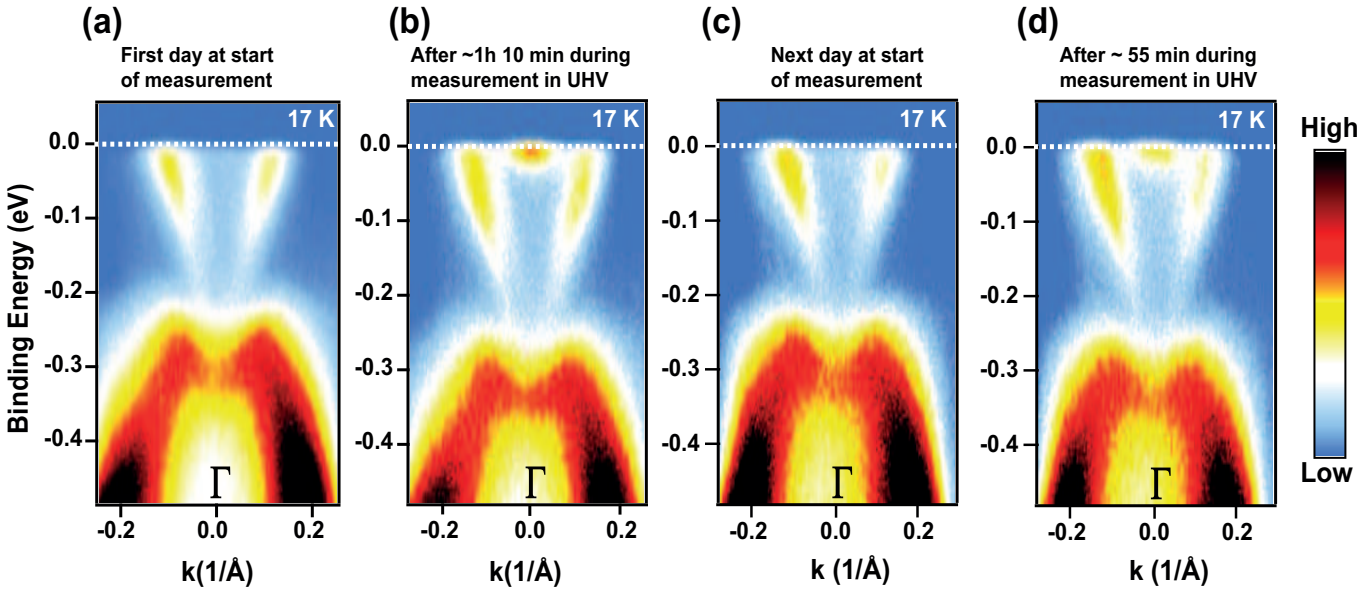

Figure S6: ARPES spectra of a 15 nm thick Bi_2Te_3 film grown on $SrTiO_3$ [111]. Measurements were taken over different time intervals in UHV conditions during ARPES measurements. (a) Only topological surface states at the Fermi level are observed at the beginning of the experiment, (b) but after $\sim$ 1h 10 min bulk conduction bands start to bend downward due to surface adsorption effect from probably the residual gases (H_2,CO, N_2). (c) Raising temperature back to room temperature and allowing the sample to recover for sometime in UHV conditions resets the amount of band bending by desorption of the adatoms. The spectrum was measured after recooling to $\sim$ 17 K (d) The downward bulk band bending reappears again after $\sim$ 55 min during low-temperature ARPES measurements. These observations further support the fact that our films do not degrade in UHV conditions.

[1] H. Zhang, C. -X. Liu, X. -L Qi, X. Dai, Z. Fang, S. -C. Zhang, Nature Phys. **5**, 438 (2009).
[2] L. He, X. Kou, and K. L. Wang, Phys. Status Solidi RRL **7**, 50 (2013).
[3] O. Eibl, K. Nielsch, N. Peranio and F. Völklein, *Thermoelectric Bi_2Te_3 Nanomaterials*, Wiley-VCH Verlag GmBh & Co. KGaA, Weinheim, Germany (2015).
[4] S. Basak, H. Lin, L. A. Wray, S.-Y. Xu, L. Fu, M. Z. Hasan, and A. Bansil, Phys. Rev. B **84**, 121401(R) (2011).